302
Antenna Positioning

Released: October 7, 2004

Document Owner:

S. D. Slobin 8-27-04

S. D. Slobin Date
Antenna System Engineer

Approved by:

A. J. Freiley 9/10/04

A. J. Freiley Date
Antenna Product Domain Service
System Development Engineer

Released by:

Signature on file at DSMS Library 10/7/04

DSMS Document Release Date

Change Log

Rev	Issue Date	Affected Paragraphs	Change Summary
Initial	10/72004	All	New Module

Note to Readers

There are two sets of document histories in the 810-005 document that are reflected in the header at the top of the page. First, the overall document is periodically released as a revision when major changes affect a majority of the modules. For example, this document is part of Revision E. Second, the individual modules also change, starting as the initial issue that has no revision letter. When a module is changed, a change letter is appended to the module number on the second line of the header and a summary of the changes is entered in the module's change log.

Contents

Contents (Continued)

Illustrations

Tables

1 Introduction

1.1 Purpose

This module describes the pointing capabilities of the antennas used by the Deep Space Network (DSN) in sufficient detail to enable a telecommunications engineer to design spacecraft missions that are compatible with these capabilities.

1.2 Scope

This discussion in this document is restricted to the mechanical limitations of the antennas, their control algorithms, and the error sources that influence the ability to point the radio frequency (RF) beam in the desired direction. Wind velocity statistics that can be used to estimate the effects of wind on antenna pointing are presented in module 105. Coverage and restrictions to coverage caused by terrain masking are discussed in module 301.

2 General Information

Antenna positioning or pointing is the process of directing the antenna beam towards the desired target. The target may be a spacecraft or radio source that is producing a receivable signal. The target may also be a spacecraft other object at a known or suspected position that is not producing a signal but to which RF energy must be directed. The antenna must keep its RF beam properly aimed for the scheduled duration of the spacecraft or other observation, often referred to as a pass.

There are two types of antenna beam pointing. The first of these is blind pointing, sometimes referred to as open loop pointing, that relies on the ability to model the direction of the antenna beam in the presence of systematic and random processes. The second is closed-loop pointing that derives corrections from the received signal. Blind pointing produces larger errors but is the only method available in the absence of a received signal or during radio science observations when the data quality would be adversely affected by closed loop positioning.

Antenna pointing is not only influenced by random errors due to wind and thermal effects, but also due to imperfect modeling of systematic pointing errors that vary unpredictably throughout the sky or along a particular path in the sky when tracking a spacecraft. Standard first-order systematic error pointing models (used for blind pointing) may not be adequate to describe “high frequency” (e.g., 2 or more cycles per 360 degrees movement in azimuth or elevation) variations in pointing.

2.1 Antenna Characteristics

The DSN employs four general types of antennas. At least one of each type antenna exists at each DSN complex. The antenna types are the 70-m antennas, the 34-m high-efficiency (HEF) antennas, the 34-m beam waveguide (BWG) antennas, and the 26-m antennas.

The 70-m and 34-m antennas employ an azimuth-elevation (AZ-EL) mount whereas the 26-m antennas employ an X-Y mount with the primary (or lower), X-axis oriented east-west.

The antennas are pointed by variable-rate servo systems that use the antenna pointing commands as input and the axis position encoders (azimuth and elevation or X and Y) as feedback. The 70-m antennas also have a *precision mode* where the main reflector is slaved to a small hour-angle/declination instrument, referred to as the *Master Equatorial (ME)*, using optical collimation techniques. The ME is mounted at the intersection of the 70-m azimuth and elevation axes in a controlled environment and on a separate foundation to eliminate vibration and other effects. Servo performance is generally a function of antenna size with higher tracking and slew rates being available from the smaller antennas. The high-speed, 34-m BWG (HSB) antenna at the Goldstone Deep Space Communications Complex (DSCC) is an exception and has the fastest tracking and slew rates of any DSN antenna. Table 1 summarizes the primary mechanical characteristics of the various antennas.

2.2 Coverage Restrictions

DSN antennas have restrictions to their coverage from two sources other than terrain masking. The first of these is the antenna *keyholes* – areas where coverage in not possible because the reflector would need to be positioned about the secondary (upper) axis in such a way that it would run into the primary (lower) axis or its supporting structure. The 26-m antennas have keyholes directly to the east and west of the antenna. The sizes of the keyholes can be inferred from the motion limits given in Table 1 and are illustrated on the horizon mask charts in module 301. The second restriction occurs near the ends of the primary axis where the amount of motion required to correctly position the antenna beam exceeds the capability of the primary axis servo should the orbital path passes near an imaginary extension of the lower axis.

2.2.1 Servo Performance Limits of Azimuth-Elevation Antennas

Azimuth-elevation antennas have an area of non-coverage directly above the antenna resulting from the fact that should a spacecraft pass directly overhead, the antenna would have to instantaneously rotate 180 degrees in azimuth to follow it. Clearly, this is not possible but, for spacecraft passing nearly overhead, the azimuth rate is finite and can be calculated from the equation.

$$r_{AZ} = \frac{r_{SC}}{\cos(EL_{Peak})} \tag{1}$$

where

r_{AZ} = the peak azimuth rate required of the antenna

r_{SC} = the cross-elevation rate of the spacecraft as seen from the antenna

EL_{Peak} = the maximum elevation reached by the spacecraft.

Table 1. DSN Antenna Mechanical Characteristics

Parameter	70-m	34-m HEF	34-m BWG	34-m HSB	26-m
Antenna Mount	AZ-EL	AZ-EL	AZ-EL	AZ-EL	X-Y
Slew Rate, each axis (deg/s)	0.25	0.8	0.8	3.0 (AZ) 2.0 (EL)	2.0
Minimum Tracking Rate, each axis (deg/s)	0.0001	0.0001	0.0001	0.0001	0.0035*
Maximum Tracking Rate, each axis (deg/s)	0.25	0.4	0.4	3.0 (AZ) 2.0 (EL)	2.0
Acceleration each axis (deg/s^2)	0.2	0.4	0.4	1.0 (AZ) 0.5 (EL)	5.0
Deceleration (braking) each axis (deg/s^2)	2.5	5.0	5.0	5.0	25.0
Axis Encoder Resolution (mdeg)	0.021	0.021	0.021	0.021	1.37
Axis Encoder Accuracy (mdeg)	±0.171	±0.171	±0.171	±0.171	±2.75
Master Equatorial Axis Encoder Resolution (mdeg)	0.021	–	–	–	–
Master Equatorial Axis Encoder Accuracy (mdeg)	±0.343	–	–	–	–
Azimuth Motion Limits from Wrap Canter (deg)	±265	±225	±225	±292	±85
GDSCC Wrap Center (deg)	45	135	135	135	0 (X)
CDSCC Wrap Center (deg)	135	45	45	–	0 (X)
MDSCC Wrap Center (deg	45	135	135	–	0 (X)
Elevation Motion Limits (deg)	6 – 89.5	6 – 89.5	6 – 89.5	5 – 89.5	±76 (Y)

* The 0.0035 deg/s lower limit is defined as smooth motion provided by the antenna mechanical and servo assemblies. “Smooth” means continuous, monotonically increasing or decreasing motion, or motion in a specific direction without stopping or reversal. The antenna controller can emulate a much lower rate through the use of stopping intervals when tracking of slower moving targets is required.

For spacecraft tracked at near-sidereal rates, the areas of non-coverage are not large but must be avoided by appropriate scheduling. The maximum peak spacecraft elevation is limited to 89 degrees for continuous tracking when using the 70-m antennas. For the HEF and BWG antennas, the maximum peak elevation for continuous tracking is limited to 89.4 degrees.

Formula (1) can be used for Earth-orbiter spacecraft; however, the rate of spacecraft as seen from the antenna will be a function of orbit altitude. Figure 1 illustrates the effect of orbit altitude on peak azimuth rate for several circular orbits.

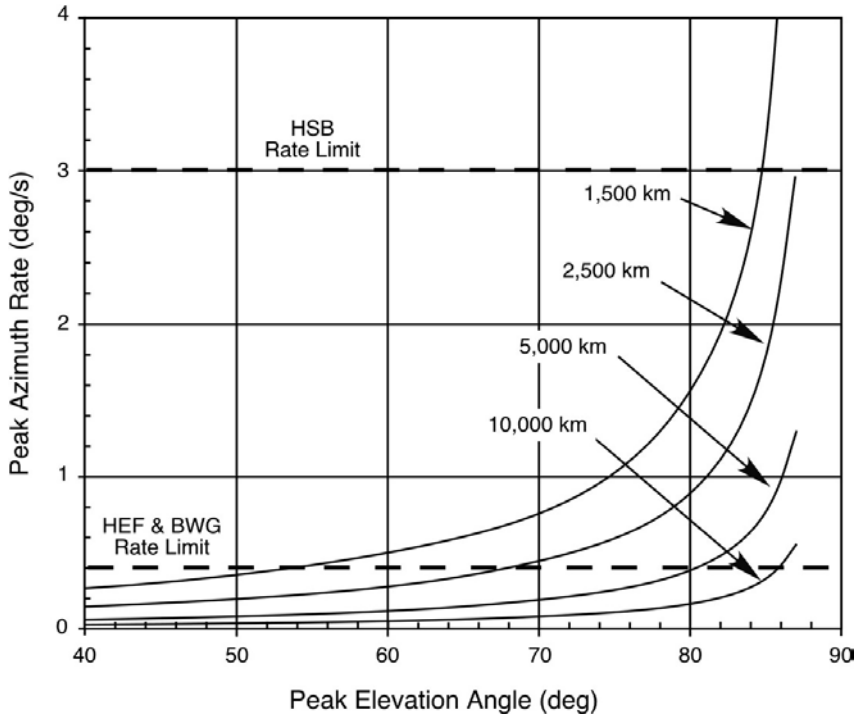

Figure 1. Azimuth Rates for Selected Circular Orbits.

2.2.2 Servo Performance Limits of the DSN 26-m Antennas

When tracking earth orbiters near the 26-m antenna east and west keyholes, the maximum X-rate (2.0 deg/s) may not be sufficient to keep up with the spacecraft. This condition occurs when the orbiter is at an altitude less than 300 km and passing just above the keyhole at an elevation angle of 14 – 20 degrees.

Figure 2 shows the maximum X-rate needed to track a polar-orbiting satellite as it passes above the eastern and western keyholes at various elevation angles. It is seen that for satellites at altitudes below 300 km, an X-rate greater than 2 deg/s may be needed for low elevation angles. For satellites with altitudes greater than 400 km, the maximum X-rate available

is sufficient to track the satellite even at the maximum Y value of 76 degrees (an elevation of 14 degrees at the eastern and western keyholes). Satellites may be tracked at lower altitudes provided they are at inclinations that share antenna movement between the two axes. Detailed calculations should be made to verify the antenna capabilities for satellites in other orbits and at different elevation angles.

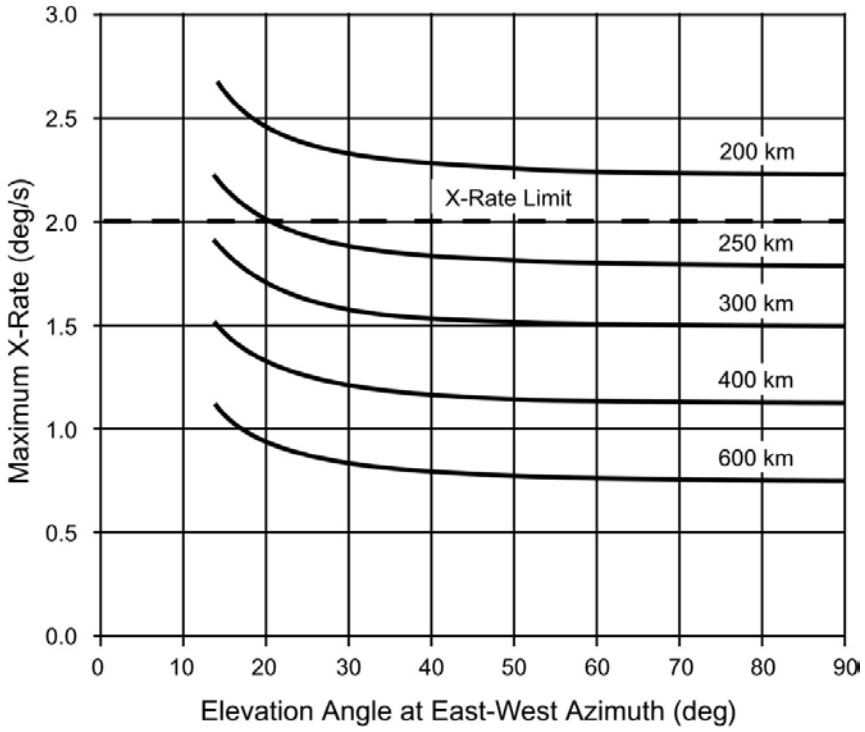

Figure 2. X Rates for Selected Polar Orbits.

2.2.3 Coordinate Conversions

Conversion between the azimuth-elevation and X-Y coordinate systems can be accomplished with the following formulas.

$$X = \tan^{-1}\left[\frac{\cos(AZ)\cos(EL)}{\sin(EL)}\right] \tag{2}$$

$$Y = \sin^{-1}\left[\sin(AZ)\cos(EL)\right] \tag{3}$$

$$AZ = \tan^{-1}\left[\frac{\sin(Y)}{\cos(Y)\sin(X)}\right] \tag{4}$$

$$EL = \sin^{-1}\left[\cos(Y)\cos(X)\right] \tag{5}$$

The sign convention is that X is positive south of the antenna and negative north of the antenna. Y is positive east of the antenna and negative west of the antenna. Azimuth is 0 at true north, positive east of north, and negative west of north. For example, if AZ = 40 degrees and EL = 50 degrees, X = –32.7 degrees and Y = +24.4 degrees. For X = 40 degrees and Y= 50 degrees, AZ = 118.3 degrees and EL = 29.5 degrees.

2.3 Pointing Modes

DSN antennas are normally operated by aiming their RF beams in accordance with a pre-determined set of instructions referred to as antenna pointing predictions or *predicts*. The format and contents of the predicts depends on their source, the type of support being provided, and the antenna being used. In addition to predict-driven modes, there are specialized pointing modes available for each antenna type. All pointing is provided in terms of the actual direction to the target. The antenna controller adds whatever corrections are required to compensate for the atmosphere and imperfections in the antenna response, calculates the rate at which each axis must move to reach the next point at the desired time and delivers this information to the antenna servos. Position feedback from the selected axis position encoders is constantly monitored and used to adjust the axis tracking rates.

2.3.1 34-m and 70-m Pointing Modes

The 34-m and 70-m antennas have two predict-driven modes and two additional pointing modes as described below.

2.3.1.1 Direction Cosine Mode

Target positions are delivered to the station as a binary file of predict points, where each point contains time, target range, and topographic direction cosines (X, Y, and Z) with their 2^{nd} and 4^{th} differences for use in an Everett Interpolation algorithm within the antenna controller. The points may represent the location of a single spacecraft from which data is to be acquired for an entire pass, a collection of radio sources that are to be observed on a pre-determined schedule, or in the case of delta-differential one-way ranging (ΔDOR), a series of observations alternating between a spacecraft and one or more radio sources.

2.3.1.2 Improved Inter-Range Vector (IIRV) Mode

The IIRV (“I-squared RV”) mode is most commonly used for tracking Earth orbiter spacecraft or deep space spacecraft during their launch and acquisition phase. Target position is expressed as a text file of state vectors in the geocentric Greenwich rotating coordinate frame. Each vector contains time and the three components of target position and velocity. The antenna controller converts the predicts to pointing commands by interpolation or integration and translates them to the coordinate system of the antenna. The time increment between predicts is normally 4 hours; however, predictions can be interpolated over intervals as small as 30 seconds and extrapolated up to 24 hours.

A special case of the IIRV mode enables a 34-m or 70-m antenna to utilize information provided by the 26-m antenna to correct the time in the predicts being used by the larger antenna. This function enables the 26-m antenna with its autotrack capability to be used as

an acquisition aid during spacecraft launch and initial acquisition. It is important to consider the lower tracking rates of the large antennas before attempting to use this capability and, of course, both antennas must be scheduled for the support activity.

2.3.1.3 Planetary Mode

Planetary mode is used to track an object with slowly varying right ascension and declination. Pointing commands are interpolated from three planetary predict points entered from the control position or read from a locally-created file of at least four predict points. The points may be geocentric or topocentric and should include nutation and precession. Each point contains time, right ascension, and range. Parallax correction is available for use with geocentric points when a non-sidereal object (such as a planet) is to be tracked.

2.3.1.4 Sidereal Mode

This mode, also called Star Track Mode, is used to track a celestial object at a fixed position described by geocentric right ascension (RA) and declination (DEC) coordinates including precession and nutation. The points may be entered from the local control position or may be read from a locally-created file containing RA, DEC, and time. A capability to boresight the antenna after arriving on point is included. The boresight algorithm performs a small cross-elevation (XEL) scan centered on the expected target location followed by a small elevation (EL) scan. Pointing corrections are estimated from signal strength measurements. This mode is mainly used for evaluating antenna performance and collecting very-long baseline interferometry (VLBI) data.

2.3.1.5 70-m Precision Tracking Mode

The 70-m antennas have a precision tracking mode that makes use of an instrument called the *master equatorial* (ME). The master equatorial is a 7-inch (17.8 cm) mirror on an hour-angle/declination mount. The mount is attached to the top of a concrete and steel tower on a separate foundation in an environmentally controlled area within the antenna pedestal and alidade structure. The mirror can be positioned to better than 1 mdeg in each axis and the 70-m reflector is optically slaved to it. The precision tracking mode is available with any of the above modes but should only be used when needed because of its extra complexity.

2.3.2 26-m Pointing Modes

The 26-m antennas have three predict-driven modes and two additional pointing modes as described below.

2.3.2.1 Improved Inter-Range Vector (IIRV) Mode

The IIRV mode is the normal mode for tracking all spacecraft at the 26-m antennas. The description for IIRV predicts is provided in paragraph 2.3.1.2.

2.3.2.2 Internet Predicts (INP) Mode

The 26-m antenna can be pointed in accordance with a file containing from 6 to 100 predict points where each point contains the X- and Y- positions of the antenna, the round-trip light time (RTLT) to the spacecraft, Doppler predictions, the day of year, and UTC (universal coordinated time) time of day.

2.3.2.3 Geocentric Predicts Mode

The 26-m antenna can be pointed in accordance with a file containing apparent true-of-date geocentric predictions of the observed signal from the spacecraft. The predictions must include the effects of precession, nutation, and annual aberrations. They should not include effects of polar motion, parallax, or tropospheric refraction. The points are equally spaced in time and each point contains the date and time in UTC, the geocentric RA, the averaged rate of change of Right Ascension (RA dot), the geocentric DEC, the averaged rate of change of declination (DEC dot), and the RTLT to the spacecraft. RTLT is required to determine parallax corrections.

2.3.2.4 Star Mode

The 26-m antenna controller contains a star catalog of up to 20 sources in RA-DEC coordinates that can be selected by whatever name is used in the catalog.

2.3.2.5 Look Angle Mode

Any of the above predict types can be converted to a table of look angles for later use in pointing the antenna.

2.3.2.6 Spacecraft Acquisition

The 26 meter antenna controller provides the ability to maintain both a primary and a backup set of predicts and the ability to bias the X and Y axis positions and time as an aid to spacecraft acquisition. The position and time biases can be entered separately for the primary and backup predicts. The axis biases are in the range of ±90 degrees. The time bias is ±366 days and ±23 hours, 59 minutes, and 59 seconds.

The controller also can add built-in or custom scan patterns to the predicted spacecraft or source trajectory. The system-provided patterns are circular, raster (perpendicular to the trajectory or parallel to the ground), and spiral. The custom scan pattern consists of a series of X, Y and duration points in a text file that is furnished by the user.

2.4 Statistics of Pointing Errors

If an antenna has EL and XEL random pointing errors due to any number of causes that are normally (Gaussian) distributed, it can be shown that for equal EL and XEL standard deviations, σ, the radial pointing error (two dimensional) becomes Rayleigh distributed. The characteristics of the Rayleigh distribution are that the probability density function (PDF) is zero at zero pointing error, rises to a maximum value at the EL and XEL σ, and decreases with a long tail out to large values of radial pointing error. The cumulative distribution (CD) of the

pointing error at a particular value is the integral of the PDF from zero to that value. The mean radial error (MRE) for the Rayleigh distribution of radial pointing errors is related to the standard deviation of the axial (XEL and EL) distributions as:

$$\mathrm{MRE} = \sqrt{\pi/2} \cdot \sigma = 1.2533\sigma \tag{6}$$

and the cumulative distribution at the MRE is 0.545. This means that 54.5% of the pointing errors are less than or equal to the MRE. Conversely, 45.5% of the pointing errors are larger than the MRE. Once the MRE is known, the radial error associated with any CD can be calculated from the properties of the Rayleigh distribution. Table 2 provides the factors by which the MRE must be multiplied to obtain the radial error at the selected CD.

Table 2. Mean Radial Error Multipliers for a Rayleigh Distribution.

CD	Mean Radial Error Multiplier	CD	Mean Radial Error Multiplier
0.0	0.000	0.6	1.080
0.1	0.366	0.7	1.238
0.2	0.533	0.8	1.431
0.3	0.673	0.9	1.712
0.4	0.806	0.95	1.953
0.5	0.939	0.98	2.232
0.545	1.000 (MRE)	0.99	2.421

Figure 3 shows a graph of the PDF and cumulative distribution function (CDF) for a Rayleigh distribution with axial (XEL and EL) σ of 3.19 mdeg, chosen to yield a mean radial error of 4.00 mdeg. Pointing performance such as this would be acceptable for a 34-m DSN antenna operating at X-band where the pointing loss (see module 104) would be less than 0.13 dB 90% of the time. It would be not be acceptable pointing for the same antenna operating at Ka-band antenna where the beamwidth is substantially smaller. The resulting Ka-band pointing loss (see module 104) would be greater than 0.7 dB, 45.5% percent of the time and greater than 2 dB 10% of the time.

Figure 4 shows cumulative distributions of pointing error for values of mean radial error ranging from 2 to 20 mdeg and includes the pointing loss curves from modules 101 (70-m Telecommunications Interfaces) and 104 (34-m BWG Telecommunications Interfaces). As an example of the use of this figure, consider the inverse of the preceding example. Assuming it has been determined that a 90% probability of having no more than 2 dB of pointing loss for a Ka-band experiment is acceptable, the chart is entered from the right along the 2-dB line until it intersects the Ka-band Pointing Loss curve. The line is extended vertically to the CD = 0.9 line where it intersects the MRE = 4 curve. Thus, to accomplish the experiment with the desired probability of success will require an antenna with an MRE capability of 4 mdeg.

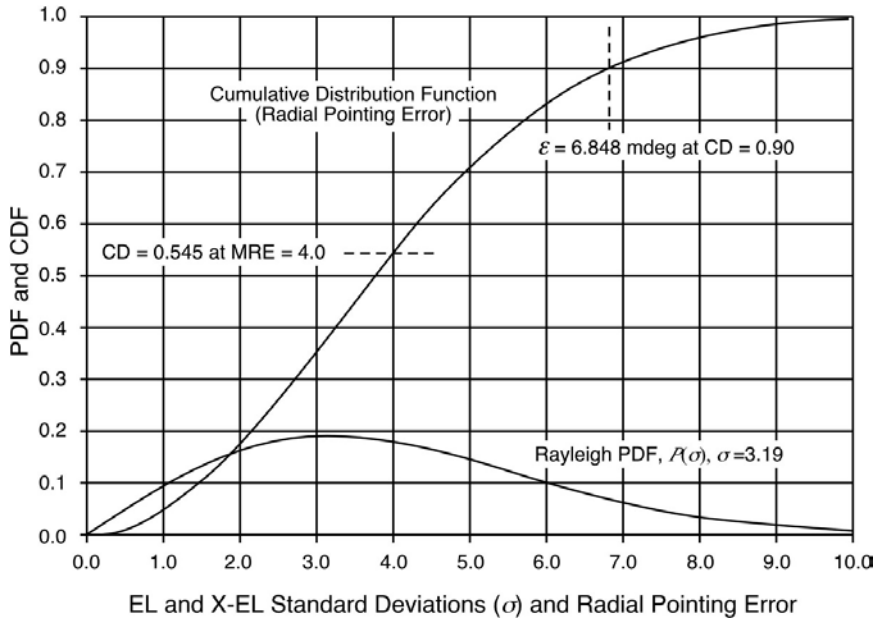

Figure 3. Rayleigh PDF and CDF for a Mean Radial Pointing Error = 4.0 mdeg.

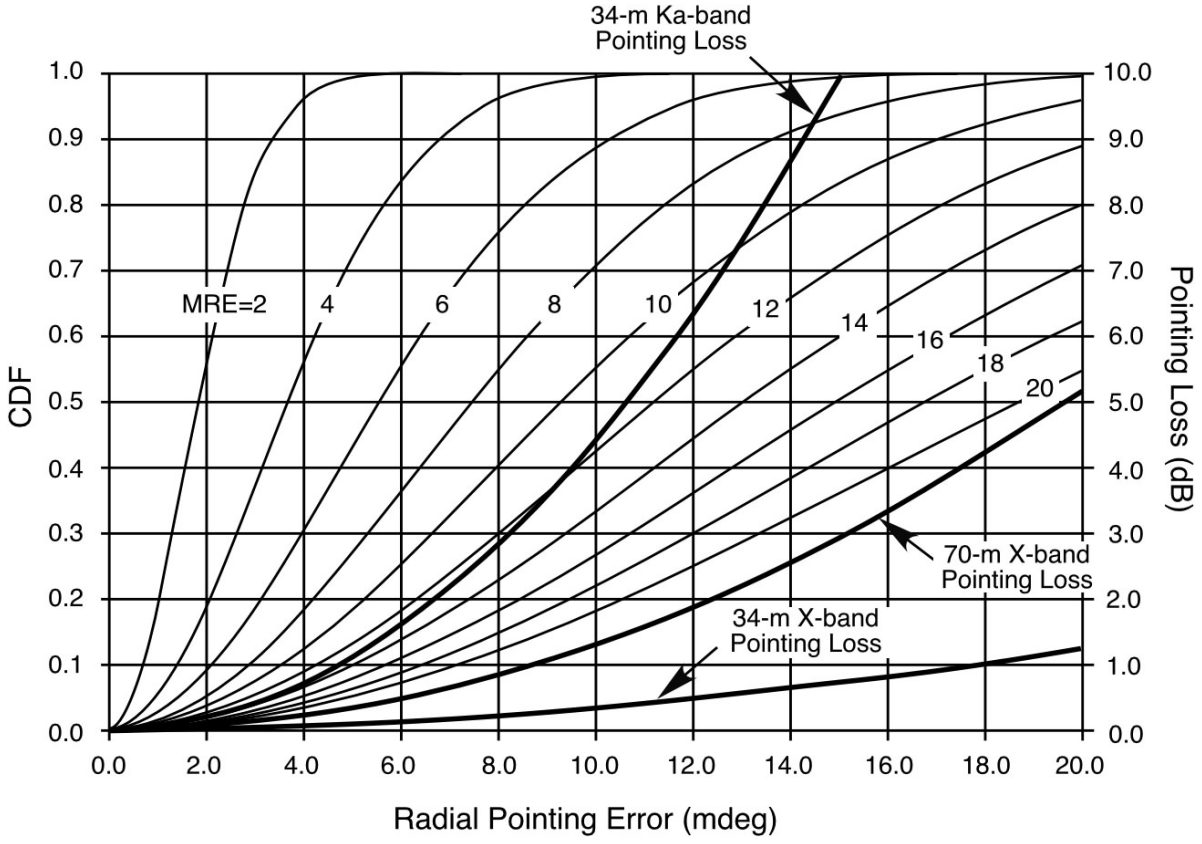

Figure 4. Cumulative Distributions of Pointing Errors for Selected MREs

2.5 Blind Pointing

Blind pointing relies on calibration and computer modeling to compensate for errors between the antenna beam direction and the direction as reported by the antenna axis position encoders. Blind pointing errors result in a pointing loss that is most severe on the BWG antennas when operating at Ka-band because of the extremely narrow beamwidth. The 70-m antennas have a relatively narrow X-band beamwidth but this is mitigated by use of the precision tracking mode. The BWG antennas' beam waveguide tube at the center of the antenna prevents use of a master equatorial, and there are additional error sources. The BWG error sources, their magnitude, and the degree to which they can be reduced by modeling are tabulated in Table 3 and discussed in the following paragraphs.

Table 3. 34-m BWG Antenna Pointing Error Sources

Error Source	Estimated Size (mdeg)	Correction Method	Residual Error (mdeg)
Atmospheric refractivity	83 at EL = 10°	Surface weather model	0.8, 1□ at EL=10°
Gravity deformation of dish and quadripod	100, EL (max)	Subreflector lookup table	5 – 10 P-P (□ 6□)
Systematic errors	100, EL (max)	12 term, first order trigonometric model	1 – 8 (range)
Azimuth track level	8 P-P (□ 6□)	Lookup table	0.3 XEL, 0.1 EL
Azimuth encoder gear noise	0.44, 1□	Uncorrected	0.44, 1□
Elevation encoder	0.2	Uncorrected	0.2, 1□
Thermal deformation	8 P-P (□ 6□, EL & XEL)	Uncorrected	8 P-P (□ 6□)
Wind displacement of foundation	1.1 (30 mph wind)	Uncorrected	1.1 (30 mph wind)
Wind distortion of structure	6 – 9 (30 mph wind)	Uncorrected	6 – 9 (30 mph wind)
Calibration measurements	1, 1□	Uncorrected	1, 1□
Mean pointing error (without wind)			2.3 – 8.4 (range)
Mean pointing error (with 30 mph wind)			6.5 – 12.4 (range)

2.5.1 Pointing Corrections

2.5.1.1 Atmospheric Refraction Correction

The antenna controller uses local surface weather measurements to calculate and apply a pointing correction in elevation to compensate for atmospheric refraction. The weather data normally is provided from a local weather station but may be manually entered, if necessary.

2.5.1.2 Gravity Deformation Correction

The main reflector and the quadripod structure that supports the subreflector change shape slightly when the antenna moves in elevation. Because of this, the subreflector must be moved continuously during a pass in both the up and down as well as the in and out directions to optimize the gain. The up-down component of the motion causes a shift in antenna pointing referred to as *squint*. This is compensated for by a squint correction algorithm that adjusts the elevation pointing depending on how far the subreflector has been moved. The 26-m and 34-m HSB S-band antennas have a fixed subreflector because of their relatively wide beamwidths and squint correction is not necessary.

2.5.1.3 Systematic Error Correction

All antennas, no matter how well they are designed and how carefully they are built, have certain repeatable pointing errors that can be measured by referencing well-known radio sources. Among the causes for these errors are imperfections such as angle-encoder offsets, azimuth axis tilt, gravitational flexure, axis skew, structure aging, etc. The DSN models these using constants and spherical harmonic functions of the antenna pointing angle in what is called a first-order pointing model. This model works reasonably well over the entire sky at S-band and X-band. However, experiments requiring extremely accurate pointing can benefit by special calibrations and adjusting the model for optimum performance in the portion of the sky where the experiment will occur. Antenna calibrations are performed periodically and the best model for the planned activity is always used.

The addition of Ka-band to the network has made the first order model inadequate as an all-sky model. As a result, a 4^{th} order systematic error model has been developed to handle pointing variations that are not directly traceable to physical imperfections in the antenna. More frequent calibration and possible use of different models for day and night operation are also being investigated to improve Ka-band pointing.

2.5.1.4 Azimuth Track Level Compensation

The BWG antenna azimuth tracks are composed of eight, precision-machined segments. Extremely small irregularities in the track, coupled with the four-wheeled rectangular support structure for the antenna, result in a 32-node signature that is more complex than can be modeled by the 1^{st} order or 4^{th} order systematic error correction model. The antenna controller employs a lookup table and applies appropriate corrections to both elevation and azimuth axes.

2.5.2 Measured Performance of DSN Antennas

Pointing performance can be observed by monitoring the corrections applied to pointing predicts during closed-loop tracking. Assuming the predicts are perfect and the antenna controller is applying corrections properly, the closed-loop residuals represent the difference between the desired beam pointing and the actual pointing – in other words, the pointing error. Figure 5 shows the X-band pointing corrections (the negative running sum of the pointing errors) as determined by conical scan (CONSCAN, see paragraph 2.6.1) measurements made by the Goldstone DSS-26 BWG antenna while tracking the Voyager I spacecraft on July 11, 2004. CONSCAN corrected the antenna pointing during the track, but there are still residual pointing errors relative to the existing systematic pointing error model (the blind-pointing model). These are presented in the figure. This represents about 5 hours of data, from an azimuth nearly southeast to shortly before setting in the west.

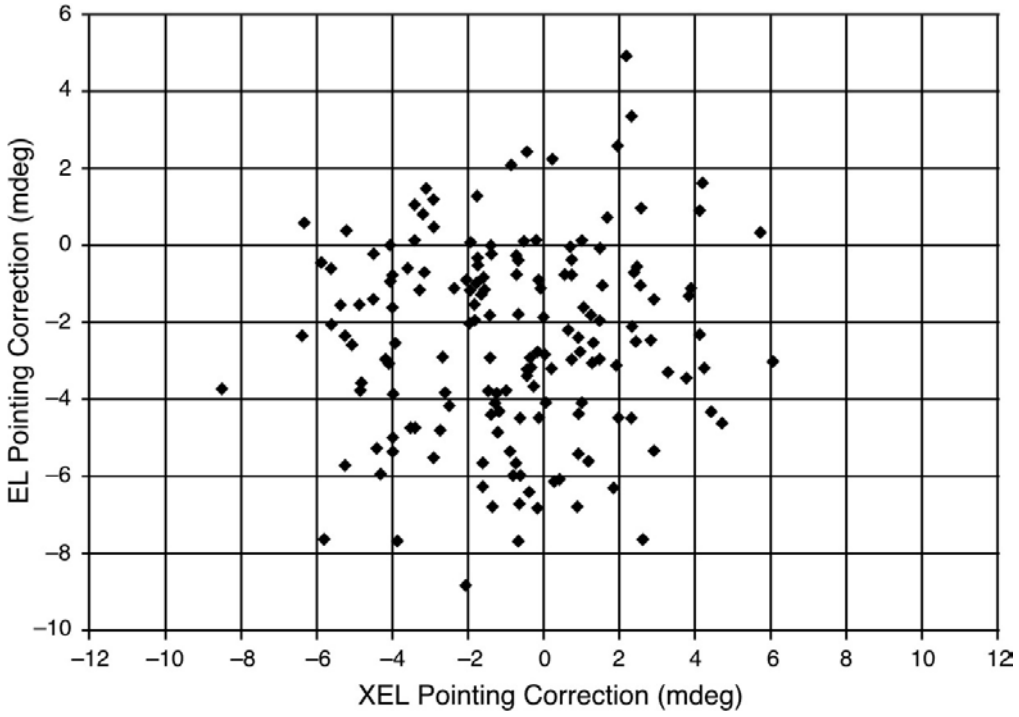

Figure 5. DSS-26 X-band Pointing Performance, July 11, 2004

From this figure it is seen that the points seem to cluster around (0, –2). The actual average XEL correction is –0.9 mdeg and the EL correction is –2.5 mdeg. The mean radial error (relative to 0, 0) for these points is 4.1 mdeg. When additional data from tracking the Cassini and Odyssey spacecraft are added to the set, the mean radial error for the total data set becomes 4.9 mdeg. This pointing performance is considered to be fairly typical of BWG antennas.

Figure 6 shows DSS-26 X-band radial pointing errors determined by open-loop CONSCAN tracks at various wind speeds while tracking the Cassini and Deep Space 1 spacecraft in December, 2001. It is been suggested that the pointing errors are a quadratic function of wind speed, although insufficient data have been collected to thoroughly investigate the relationship. The large pointing errors (above 8 mdeg) at low wind speeds (below 5 mph) are believed to be due to thermal effects on the antenna alidade and main reflector structure as the morning sun shone on the back of the antenna. Excluding those points and the high wind speed points, it is seen that the mean radial error for this data set is below 4 mdeg.

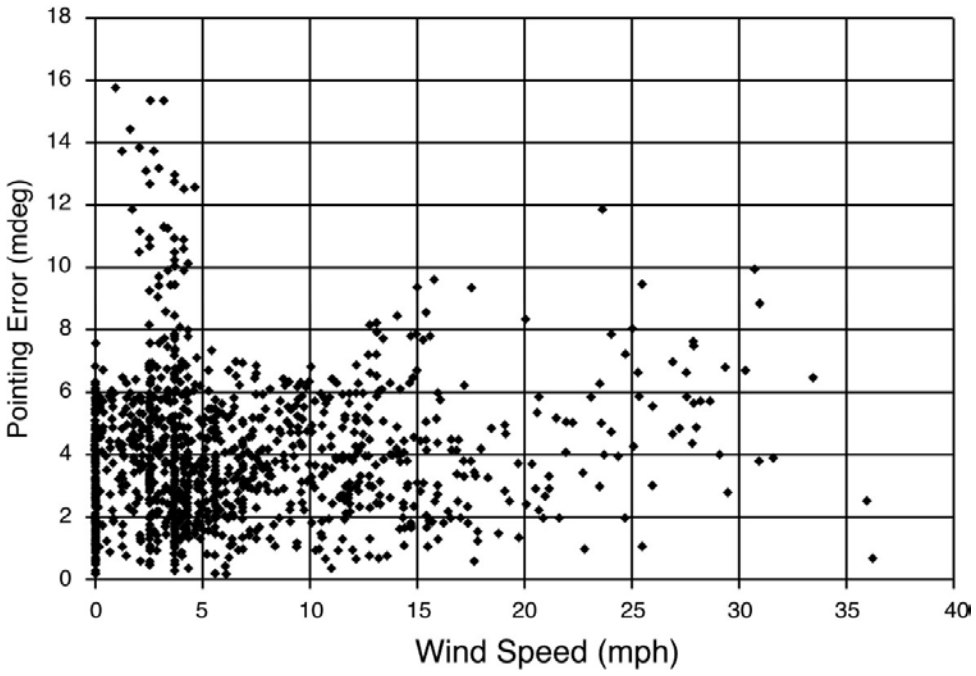

Figure 6. DSS-26 X-band Pointing at Various Wind Speeds

Table 4 presents measured X-band blind-pointing pointing performance of DSN antennas. Insufficient data have been acquired to give a proper assessment of pointing at Ka-band. S-band pointing is not provided as X-band pointing models are good enough to be used for S-band, due to the much large S-band beamwidth.

2.6 Closed-loop Pointing

Closed-loop pointing relies on the signal being received to provide corrections for antenna pointing. The DSN employs two methods of closed-loop pointing, CONSCAN and monopulse.

Table 4. Measured Blind Pointing Performance of DSN Antennas

Antennas	Mean Radial Error, mdeg	Remarks
70-Meter		
DSS-14, Goldstone	1.67, precision mode (ME)	limited data set, 4/2004
DSS-43, Canberra	3.04, precision mode (ME) 6.19, normal mode	10/2002-12/2003
DSS-63, Madrid	1.37, precision mode (ME)	limited data set, 3/2004
34-Meter HEF		
DSS-15, Goldstone	TBD	data not available
DSS-45, Canberra	6.69	1/2003-12/2003
DSS-65, Madrid	3.66	limited data set, 3/2004
34-Meter BWG		
DSS-24, Goldstone	TBD	data not available
DSS-25, Goldstone	7.50	9/2003-10/2003
DSS-26, Goldstone	4.91	7/2004
DSS-34, Canberra	6.53	9/2003-12/2003
DSS-54, Madrid	4.81	limited data set, 2/2004
DSS-55, Madrid	4.34	limited data set, 3/2004
34-Meter HSB		
DSS-27, Goldstone	TBD	data not available
26-Meter		
DSS-16, 46, 66	TBD	data not available

2.6.1 CONSCAN

CONSCAN is available on the 70-m antennas and all 34-m antennas except the 34-m HSB antenna. It consists of performing a circular scan (as seen from the target) with the center at the predicted source position and a radius that reduces the received signal level by a small amount, typically 0.1 dB. If the target is at the expected location and antenna pointing is perfect, no variation in the received signal level will be detected. If the initial pointing is imperfect or the target is not at the predicted location, each CONSCAN cycle will see a variation in amplitude from which the radial error and clock angle of the mis-pointing can be calculated. The typical time for a CONSCAN cycle is 120 seconds and the pointing is corrected after each cycle. The process is repeated continuously during the pass. Various amounts of CONSCAN

"gain" can be applied for making the pointing correction, ranging from 0 (no correction applied) to 1 (full detected correction applied). A gain of less than 1 is usually applied to reduce the effect of noise during the CONSCAN cycle. This results in some time delay (perhaps 20 minutes) before fully corrected pointing is obtained.

CONSCAN is available at all frequency bands but is usually not necessary at S-band and is not recommended for Ka-band. The relatively long CONSCAN cycle coupled with the much more severe Ka-band atmospheric effects can provide misleading information to the pointing correction algorithm resulting in the antenna being driven off-point.

The mean pointing error (used for estimating pointing loss) using CONSCAN should be considered as the 0.1 dB point on the antenna pattern for the antenna and frequency in question. For a 34-meter antenna at X-band, this value is 6 mdeg and for a 70-meter antenna at X-band it is 3 mdeg. Considering CONSCAN pointing to be Rayleigh distributed, the pointing error for various CDs can be calculated or extracted from Figure 4. Antenna beam patterns for the various DSN antennas are given in modules 101 through 104.

For making pointing measurements using radio sources, a CONSCAN radius yielding a 3-dB pointing loss is often used as this gives greater sensitivity to small pointing errors than the smaller radii used for spacecraft tracking. Analysis shows that, with the exception of extremely strong radio sources, the optimum tracking of radio sources will occur when the ratio of scan radius to half-power beamwidth equals 0.425. This causes a reduction in effective antenna gain of 2.17 dB and a mean pointing error of 28 mdeg for a 34-m antenna at X-band. The mean pointing error for an X-band 34-m antenna at the 3-dB point is at 0.033 deg. The equivalent mean pointing errors for the 70-m antennas are 0.016 deg at the 3-dB point and 0.14 deg for optimum tracking.

2.6.2 Monopulse

Monopulse is a technique for extracting pointing information from the phase of the received signal while maintaining the source at the peak of the antenna pattern. The DSN employs two different techniques to recover this information. Both methods rely on the presence of a carrier signal to provide a reference for the error channel(s). As a result, the existing implementations are not suitable for suppressed carrier signals or radio sources.

2.6.2.1 Monopulse on the 26-m Antennas

The 26-m antennas have a 4-horn amplitude monopulse feed where the feeds are combined to produce a single sum pattern and two difference patterns – one aligned with each antenna axis. The signal in each difference or error channel is zero when the antenna is on point for that axis and increases as the signal moves away from the null with the error channel phase indicating the direction.

Target motion introduces a tracking error with a magnitude dependent on the selected servo loop characteristics and target velocity and acceleration. The primary mode of operation employs a second-order servo loop that eliminates tracking error for constant-velocity targets. A first-order loop is also available that minimizes overshoot when performing acquisition using scan patterns or by intercepting the signal. In the primary mode, the effect of

reducing servo bandwidth is to place restrictions on the amount of target acceleration which can be accommodated by the servo system. In the secondary mode (i.e., when using the first-order loop), the effect of reducing servo bandwidth is to place restrictions on the maximum target velocity. Table 5 lists the maximum target acceleration and velocity as a function of the available servo bandwidths.

Table 5. Maximum Target Acceleration and Velocity for 26-m Monopulse Tracking

Servo Bandwidth (Hz)	Maximum Acceleration (Second-order Loop)	Maximum Velocity (First-order Loop)
1.0	5.0 deg/s^2	3.0 deg/s*
0.5	2.5 deg/s^2	1.5 deg/s
0.25	1.25 deg/s^2	0.75 deg/s
0.125	0.62 deg/s^2	0.37 deg/s

* Limited to 2.0 deg/s in each axis by servo performance.

The 26-m antenna has two small reflectors equipped with monopulse feeds and mounted on the edge of the main reflector to serve as acquisition aids. One of these operates at S-band and utilizes the same receiver as the main reflector. This enables telemetry to be processed when using the S-band acquisition antenna. The second operates at X-band and has an independent receiver that does not process telemetry. As a result, the 26-m station performs the tracking and relays predict biases to a 34-m or 70-m antenna where the X-band telemetry is received as discussed in paragraph 2.3.1.2, The characteristics of the 26-meter acquisition aids are given in module 102.

2.6.2.1 Monopulse on the 34-m Antennas

The 34-m BWG antenna Ka-band feeds include a cryogenically cooled TE_{21} mode coupler that extracts a signal whose phase, with respect to the main beam signal, indicates the direction of the target with respect to the center of the beam and whose amplitude indicates the angular displacement from the beam center. The advantage of such a system over a conventional amplitude monopulse system is that only a single receiver channel is required for the error signal as opposed to two. The monopulse receiver measures the phase and amplitude of the signal in the error channel, calculates elevation and cross-elevation corrections, and forwards this information to the antenna controller 25 times a second. The antenna controller translates the errors into the local antenna coordinate system, integrates them, and applies the corrections to the predicted azimuth and elevation positions. Initial tests on the Cassini spacecraft during cruise indicate Ka-band monopulse tracking performs to an accuracy of better than 2 mdeg.

For initial acquisition using blind pointing, monopulse seems to “pull-in” when the pointing is within about 10 mdeg. For larger pointing errors and/or low signal to noise ratios (SNRs), CONSCAN is used to get on target.

For extremely high signal-to-noise ratios (SNR > 40 dB-Hz), the monopulse system is capable of pointing the antenna within 1 mdeg of a stationary target. As SNR decreases, this performance is degraded by servo jitter resulting from noise in the selected servo bandwidth. A study has shown that the mean radial error using monopulse varies with SNR approximately as

$$MRE = 0.2 + 12e^{-0.13SNR} \text{ , mdeg} \quad (7)$$

where SNR is the monopulse signal-to-noise ratio, dB-Hz (signal in the main channel divided by noise in the error channel). For example, for SNR = 20 dB-Hz, MRE = 1.1 mdeg. SNRs below 10 dB-Hz will probably yield unacceptably poor pointing performance.

2.7 Beam Alignment

Most DSN antennas that support more than one frequency accomplish this by having multiple feedhorns. The exceptions to this are the 34-m HEF antennas that have a single S- and X-band coaxial feedhorn and the BWG antennas (with the exception of DSS-25) where there is a coaxial X- and Ka-band feedcone. When multiple feedcones are used, it is likely that there will be a small misalignment between the peak of the two antenna beams. However, if good pointing is achieved at the higher frequency, it virtually guarantees nearly perfect performance at the lower frequency due to the larger beamwidth. For example on the DSS-43, 70-m antenna (Canberra), the S- and X-band beams have a pointing difference of about 4 mdeg in the EL direction. Because the S-band beam has a half-power beamwidth of about 118 mdeg, perfect pointing at X-band would give an S-band pointing loss of less than 0.02 dB.

2.8 X-band Beam Shift on 70-m Antennas

The 70-meter antennas have an S/X dichroic plate that is retractable to provide an X-band only low-noise mode. There is an 8.5 mdeg (approximately) beam movement in the negative XEL direction (to the left, when looking outward from the antenna) when it is retracted. Separate systematic error models are maintained for each position of the dichroic plate and are selected automatically by the antenna controller.

2.9 DSS-25 Ka-band Transmit Aberration Correction

The extremely narrow beamwidth at Ka-band requires that the DSS-25 Ka-band uplink signal be aimed at the RA and DEC where the spacecraft will be when the signal arrives, while simultaneously receiving a signal that left the spacecraft one light-time previously. This is accommodated by mounting the Ka-band transmit feed on a movable X-Y platform that can displace the transmitted beam as much as 30 mdeg from the received beam. The reduction in gain caused by the feed not being located at the optimum focus of the antenna is discussed in module 104.